August 1998

ELSEVIER

Materials Letters 36 (1998) 271–278

MATERIALS LETTERS

Short-range order and atomic arrangement in the semiconducting glassy $Sb_{0.05}As_{0.45}Se_{0.50}$ by X-ray diffraction

C. Corredor [a], J. Vázquez [a,*], R.A. Ligero [b], P. Villares [b], R. Jiménez-Garay [a]

[a] *Departamento de Física de la Materia Condensada, Facultad de Ciencias, Universidad de Cádiz, Apartado 40, Puerto Real, Cádiz, Spain*
[b] *Departamento de Física Aplicada, Facultad de Ciencias, Universidad de Cádiz, Apartado 40, Puerto Real, Cádiz, Spain*

Received 29 October 1997; revised 28 January 1998; accepted 30 January 1998

Abstract

The radial distribution function (RDF) of the semiconducting glassy alloy $Sb_{0.05}As_{0.45}Se_{0.50}$ was obtained by X-ray diffraction. Once the hypotheses on the local order of the alloy had been formulated, the RDF analysis made it possible to evaluate them, referring specifically to the coordination of the antimony. On this basis, and using the semi-random Monte Carlo method, a structural model was generated whose calculated RDF would agree with the experimental RDF. From this model, structural parameters, such as atomic distances and bond angles between the different possible pairs of atoms were deduced and are proposed as a good statistical description of the glass under study.

PACS: 81.05.Ge; 81.05.Kf

Keywords: Glassy alloy; Sb–As–Se X-ray diffraction; Radial distribution function; Local order; Structural model

1. Introduction

In the last decades, liquid and amorphous semiconductors have been the subject of intense study prompted by fundamental and technological interest [1]. Despite substantial progress, one of the basic problems remains—a quantitative characterization of the atomic disorder [2]. Experimentally, the presence of disorder means that one can measure only averaged properties and an accurate determination of the individual atomic coordinates is impossible. Theoretically, non-crystalline semiconductors are particularly difficult to model, since the interatomic interactions that are responsible for short-range order (SRO), depend strongly on atomic and chemical environment. This is crucial in understanding impurity incorporation and alloying, but, even in the case of pure elemental systems, the atomic environment may change dramatically from one disordered form to another.

Chalcogenide glasses with polyvalent elements exhibit properties which are the result of the formation of three-dimensional structural units. These polyvalent atoms, which stabilize the chalcogenide structures, are preferably arsenic and germanium, which form space units with the chalcogen elements, break their characteristic complex structural formations and contribute to the establishment of more

* Corresponding author.

00167-577X/98/$19.00
PII S0167-577X(98)00055-X

homogeneous structures for the glassy alloys belonging to this type of system, a fact which explains some of their properties.

This work analyses the local order of the semiconducting glassy alloy $Sb_{0.05}As_{0.45}Se_{0.50}$ from the radial distribution function (RDF) determined through X-ray diffraction. The experimental value of the area under the first RDF peak was compared to that obtained theoretically [3–5] as a function of the coordination number of antimony and taking into account that the products of the atomic scattering factors $R_{ij}(s) = f_i(s)f_j(s)/[\sum x_i f_i(s)]^2$, depend on the scattering angle [6] and cannot always be approximated by a constant value $Z_iZ_j/(\sum x_i Z_i)^2$. Based on the above analysis and on the geometrical restrictions imposed by the experimental RDF, a spatial atomic distribution model was generated, using the Monte Carlo random method. An analysis of the main parameters of the model (coordinations, bond lengths and angles) shows good agreement with the values quoted in the literature for similar alloys.

2. Manufacturing the alloy and preparing the samples for measurement

The alloy to be studied was prepared in bulk, from its highly pure (99.999%) constituent elements, which were mixed homogeneously in adequate proportions, after being pulverized in an agate mortar to grains less than 64 μm in diameter. The powder obtained was introduced into a quartz ampoule, and submitted for 2 days to an alternating He filling and emptying process, in order to ensure the absence of oxygen inside the ampoule. After the last emptying in which a value of 10^{-4} Torr (10^{-2} N m^{-2}) was reached, the capsule was sealed with an oxyacetylene burner, and put into a furnace at 950°C for 24 h, submitted to a longitudinal rotation of $1/3$ rpm in order to ensure the homogeneity of the molten material. It was then immersed in a receptacle containing water, in order to solidify the material quickly, at an estimated quench rate of 10^2 K s^{-1}, avoiding the crystallization of the compound. The ampoule was attacked with hydrofluoridic acid until the quartz walls were weak enough to be broken with a slight pressure without affecting the material inside, a bright grey cylindrical ingot was thus obtained, which presented a large concoidal fracture, typical of amorphous materials. The obtained product later proved to be fragile, thus endorsing the method used to extract the sample from the ampoule. If the hammer-and-anvil method, widely used for more resistant alloys, had been used, it would have been impossible to extract the material intact, or even pieces large enough to carry out trustworthy measurements of its density or to make suitable bricks for doing electrical measurements.

Although the material was relatively fragile, a little piece of the alloy was carefully cut, using a diamond saw, without breaking the rest of the ingot, in order to measure its density using a pycnometric method, a value of 4.6 ± 0.1 g cm^{-3} was obtained, which is slightly under the theoretical value (5.3 g cm^{-3}) calculated for the alloy from its composition, this difference is justified by the manufacturing method, which favours the formation of microcavities inside the material. The dimensions of the cavities observed by electron microscopy range from 0.15 μm to 0.25 μm. Another piece of the ingot was reduced to powder and sifted to grains under 64 μm in diameter, and a $20 \times 20 \times 1$ mm^3 brick was made, using a hydraulic press which compressed the material for 10 h, progressively, up to 10^5 N cm^{-2}. This brick was treated with MoK_α radiation in an automatic Siemens D-500 X-ray diffractometer, in a scan at a constant angular rate, in order to confirm the amorphous nature of the material. The intensities of the radiation diffracted by the sample were obtained through four series of measurements carried out in the $6° \leq 2\theta \leq 110°$ range, two for increasing and two for decreasing scattering angles, using an angular interval of 0.2° in the 6–70° scan and of 0.5° in the 70–110° scan. These measurements were done fixing the number of counts at 4000, and digitally registering the time it took to detect them. The average value of the four measurements was taken as the radiation intensity at each observation point.

3. Obtaining the radial distribution function. Local order hypothesis

The observed intensities were corrected, as usual, for background, polarization, absorption and multiple scattering [7], in order to eliminate the portion of

radiation which does not carry structural information. The correction of incoherent intensities and the determination of the interference function make it necessary to express the experimental intensities in electron units (e.u.), as the atomic factors and Compton intensities are tabulated in these units. The normalization to electron units was done using the high angle technique [7], and the normalized intensities were corrected for the Compton component, obtaining the spectrum of coherent intensities $I_{\text{e.u.}}(s)$ used to determine the interference function

$$F(s) = s \cdot i(s) = s \frac{I_{\text{e.u.}}(s) - \sum_i x_i f_i^2(s)}{\left[\sum_i x_i f_i(s)\right]^2} \qquad (1)$$

where x_i and $f_i(s)$ are the atomic fraction and the scattering atomic factor of element i in the alloy. The function $F(s)$ was extended up to $s_{\max} = 30$ Å^{-1}, in order to avoid the spurious oscillations which appear in the RDF when small values of r are considered, due to the lack of experimental data for high values of s. The extension was done using the method described by d'Anjou and Sanz [8], based on the one proposed by Shevchik [9]. A Fourier transformation was applied to the extended interference function, obtaining the radial distribution function

$$4\pi r^2 \rho(r) = 4\pi r^2 \rho_o + rG(r) \qquad (2)$$

where ρ_o is the average experimentally measured density of the material, $\rho(r)$ represents the local atomic density affected by the Fourier transformation of products $R_{ij}(s)$, and the function $G(r)$ is given by

$$G(r) = \frac{2}{\pi} \int_0^{s_{\max}} F(s) \sin(sr) \, \mathrm{d}s \qquad (3)$$

The experimental RDF, shown in Fig. 1, supplied the structural information given in Table 1. The interval defined by the first RDF peak, corresponding to the distances between first neighbours, is such that bonds are possible between all pairs of elements in the material.

A parameter of great interest, when postulating short-range models of a glassy solid, is the area enclosed under the first RDF peak, as it represents

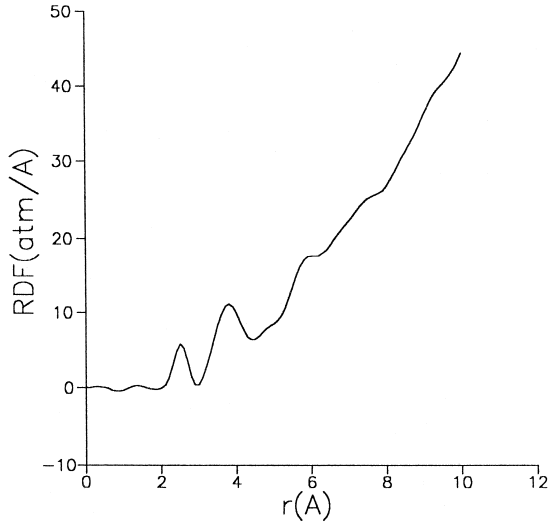

Fig. 1. Radial distribution function.

the average coordination number of the material. Bearing in mind the physical meaning of this area, and the fact that the products $R_{ij}(s)$ are functions of the scattering angle, Vázquez and Sanz [6], following the method described by Warren [7], deduced that the area under the first RDF peak is related to certain structural parameters, the relative coordination numbers n_{ij}, through the expression

$$\text{Area} = \frac{2}{\pi} \sum_i \sum_j x_i \frac{n_{ij}}{r_{ij}} \int_a^b r P_{ij}(r) \, \mathrm{d}r \qquad (4)$$

where r_{ij} is the average distance between an i-type atom and a j-type atom, a and b are the limits of the first RDF peak, and $P_{ij}(r)$ is a function defined by

$$P_{ij}(r) = \frac{1}{2} \int_0^{s_m} R_{ij}(s) \left[\cos s(r - r_{ij})\right] \mathrm{d}s \qquad (5)$$

where s_m is the upper limit of the measurement.

The structural information obtained by analyzing the experimental RDF, together with the physical–chemical properties of the alloy and of their constituent elements, make it possible to postulate the nature of the local order of the glassy materials. These hypotheses, which are reflected in the relative coordination numbers and, therefore, in the number of chemical bonds, a_{ij}, between the different pairs of elements in the material, have made it possible for

Table 1
RDF characteristics

	Maximum	
	1	2
Position (Å)	2.45	3.75
Limits (Å)	2.05–2.90	3.05–4.35
Averaged angle (deg.)	99.8	
Area (atoms)	2.57	7.23
Error	±0.1	±0.2

Vázquez el al. [5] to deduce the following relation from Eq. (4):

$$\text{Area} = \frac{1}{50\pi}\left[(h + \beta A_{22} - \delta Q)N + \alpha A_{22} + \gamma Q + P\left(\sum_{i=j\neq 1} A_{ij} - \sum_{ij\neq 1, i\neq j} A_{ij}\right)a_{ij}\right] \quad (6)$$

where h, α, β, γ and δ [5] are parameters that depend on the alloy and on the coordination hypotheses, N is the coordination attributed to a certain element in the material, P is a parameter equal to 2 when, in the variable a_{ij}, $i=j$ and equal to -1 if $i\neq j$, and A_{ij} is determined by:

$$A_{ij} = \frac{1}{r_{ij}}\int_a^b rP_{ij}(r)\,\mathrm{d}r \quad (7)$$

being

$$Q = \delta_{ij}\sum_{\substack{ij\neq 1\\ i\neq j}} A_{ij} + (1-\delta_{ij})\sum_{i=j\neq 1} A_{ij}$$

(δ_{ij} = Kronecker's delta).

This work evaluates parameters A_{ij} by adjusting functions $R_{ij}(s)$ by the corresponding straight regression lines thus obtaining the values shown in Table 2, which were calculated through the method described by Vázquez and Sanz [6]. The distances between the different pairs used are also shown in Table 2, together with the corresponding references.

In order to express the area under the first RDF peak as a function of the coordination, N, assigned to the antimony atoms in this alloy, the characteristic parameters ($h = 16.5447$, $Q = 2.9808$) where calculated according to literature [5]. The generation of local order models of the alloy $Sb_{0.05}As_{0.45}Se_{0.50}$ involves the establishment of the average coordinations of its constituent elements, which implies attributing a certain coordination to the antimony. This element may be three-fold-coordinated in the alloy under study, according to the behaviour proposed for the considered element in the literature [12,13]. In this case, the parameters, which depend on the coordination hypotheses ($\alpha = 35$, $\beta = 0$, $\gamma = 100$, $\delta = 0$) where obtained [5]. From these data, the tabulated A_{ij} and using Eq. (6), the following expression was obtained.

$$\text{Area} = 2.5251 + 10^{-4}a_{33} \quad (8)$$

and used for postulating the short-range order of the alloy. This relation may be observed to be function of the number of Se–Se bonds, a_{33}. In addition, the relative coordinations (n_{ij}, i,j, $\neq 1$) were determined according to the number of Se–Se bonds [5], resulting in the following expressions:

$$n_{22} = (35.75 + 2a_{33})/45$$

$$n_{23} = (92.5 - 2a_{33})/45$$

which also depend of the quantity a_{33}.

The theoretically calculated relative coordinations n_{22} and n_{23} must obviously be positive, a fact which restricts the number of Se–Se bonds present in the alloy for the formulated coordination hypothesis. In the case Sb three-coordinated, the interval of values in which a_{33} may oscillate is $0 \le a_{33} \le 46.25$. On the other hand, the theoretical area consequently deduced through the formulated hypothesis, Eq. (8), must be compatible with the experimental value of the abovementioned area of the first RDF peak, considering the estimated margin of error. This coherence implies a second restriction in the acceptable values of a_{33}. In the present case, the experimental area was obtained as 2.57 ± 0.1 atoms.

Table 2
Bond lengths and A_{ij} parameters

Pair	r_{ij} (Å)	Reference	A_{ij}
Sb–Sb	2.80	[10]	3.3369
Sb–As	2.60	[10]	2.4130
Sb–Se	2.56	[10]	2.3909
As–As	2.49	[11]	1.3980
As–Se	2.38	[10]	1.4904
Se–Se	2.34	[10]	1.5924

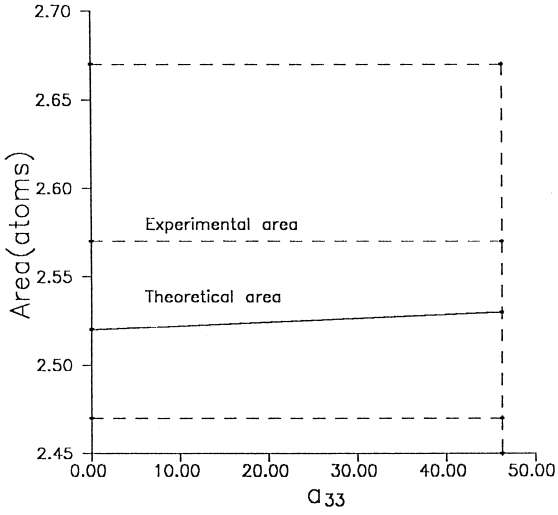

Fig. 2. Theoretical area of the first RDF peak vs. the number of Se–Se bonds for the glassy alloy $Sb_{0.05}As_{0.45}Se_{0.50}$.

The superposition of both restrictive conditions for a_{33} finally leads to the conclusion that the variation interval for the number of Se–Se bonds, in three-coordination hypothesis for the element Sb is precisely, [0–46.25].

In order to illustrate our calculations, Fig. 2 shows the theoretically calculated area vs. the number of Se–Se bonds for the antimony coordination hypothesis in glassy alloy $Sb_{0.05}As_{0.45}Se_{0.50}$. This figure shows the variation interval of a_{33} in which the theoretical area is simultaneously compatible with the experimental area and with the corresponding coordination numbers.

An analysis of the variation interval leads to the conclusion that in this alloy, the three-coordinated antimony hypothesis is compatible with the structural information obtained from the experimental data. Therefore, the most probable short-range order may be described as a three-dimensional network of covalent bonds, arranged three-fold-coordinated around antimony and arsenic atoms.

4. Structural model

There are several random methods for generating structural models of glassy materials [14–17], whose results depend on the manufacturing process used. In this work, a Monte Carlo method [18,19], described at length by Vázquez et al. [20], based on a random statistical process, was used, as it has proven to be the most suitable for glasses obtained by quenching liquids.

An initial model is taken as a starting point a spherical volume inside which the corresponding number of atoms, derived from the experimental density measured for the sample, are placed. The positions of these atoms are totally random, apart from the restrictions deduced from the experimental RDF analysis, such as the number of atoms in the first coordination sphere, the bond angle between the atoms, or the probability of bonds forming which are compatible with the formulated hypotheses, for the different elements in the alloy. Once the initial configuration is thus obtained, it is possible to calculate its RDF, taking an arbitrary atom as reference, measuring the number of atoms of each king at predetermined distances from the first, and repeating the process until all the atoms present in the adopted volume have been taken as a reference. In this way, a distance distribution function is obtained, in which the atoms occupy stationary positions, which is incorrect, as the atoms vibrate around such positions. In order to consider this fact, each averaged distance was substituted by a Gaussian distance distribution.

On the other hand, the RDF thus calculated corresponds to a spherical sample, whereas the experimental RDF was obtained by irradiating a flat sample. In order to make both functions converge, the experimental RDF was modified as proposed by Mason [21], making both RDFs comparable.

The RDF calculated for the initial model will obviously not satisfactorily approach the experimental RDF, so we proceeded to the model refining process, which basically consists of eliciting a positional variation in a given module, in a randomly chosen direction and a randomly chosen atom. The new position is accepted if, respecting the restrictions imposed in the initial configuration, derived from the RDF analysis, the new calculated RDF improves its approximation to the experimental RDF, for example through an evaluation of the mean square deviation between them. The displacement module is determined by taking into account its physical meaning, and it is modified throughout the refining process when, for a given value, the mean square devia-

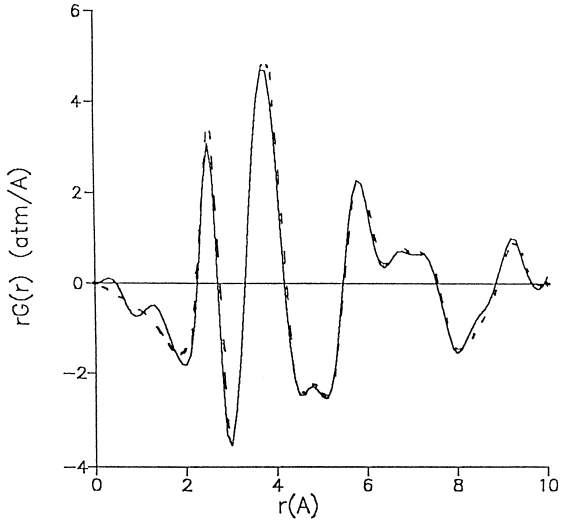

Fig. 3. Representation of experimental (————) and calculated (---) reduced RDFs.

tion between the two RDFs does not noticeably diminish.

The structural model obtained after the refining process supposes, in any case, a static atomic distribution, and the positions found for the atoms after refining must be considered as average positions around which the corresponding atoms oscillate in amplitudes depending on temperature. The thermal agitation effect is taken into account, according to the Debye–Waller model, including the thermal factor in the intensity in electron units.

For the alloy $Sb_{0.05}As_{0.45}Se_{0.50}$, 200 positions were generated, included in a 10 Å radius spherical volume, then eliminating the positions with the lowest coordination, leaving the exact number of atoms of each element, compatible with the formulated hypotheses. The elements Sb and As were assigned coordination three, and Se was assigned coordination two.

The model refining process was begun with movements of 0.5 Å and after 258 valid movements, the square deviation between the RDF of the model and the experimental RDF was 0.0423; the movements were then reduced to an amplitude of 0.3 Å. After 103 movements, the square deviation was 0.0317, and practically constant in the last 10, so it was decided to reduce the atomic movements to 0.1 Å. Once 98 movements were done, the square deviation was 0.0172, and the time used to find a valid movement was very long, so it was decided to go on to refining the thermal factors, after which the square deviation was reduced to 0.0170.

Fig. 3 shows the experimental and model-reduced radial distribution function, and Table 3 shows the initial atomic configuration and the final configuration of the generated model.

Fig. 4 shows a spatial view of the proposed model, from which the bond distances between the different atoms were deduced as shown in Table 4, as well as the average bond angles for each element in the alloy, as shown in Table 5.

It is important to note that, as is typical of the glass manufacturing methods, obvious dangling bonds appear in the proposed model. This fact reveals the presence of atoms with unsaturated bonds, and which can be partly explained by the finite

Table 3
Initial and final atomic configuration of the generated model

Element	Coordination	Number of atoms		
		Initial configuration	Final configuration	Total
Sb	3	7	7	7
As	3	66	39	66
	2	0	19	
	1	0	7	
	0	0	1	
Se	3	0	4	74
	2	74	51	
	1	0	17	
	0	0	2	

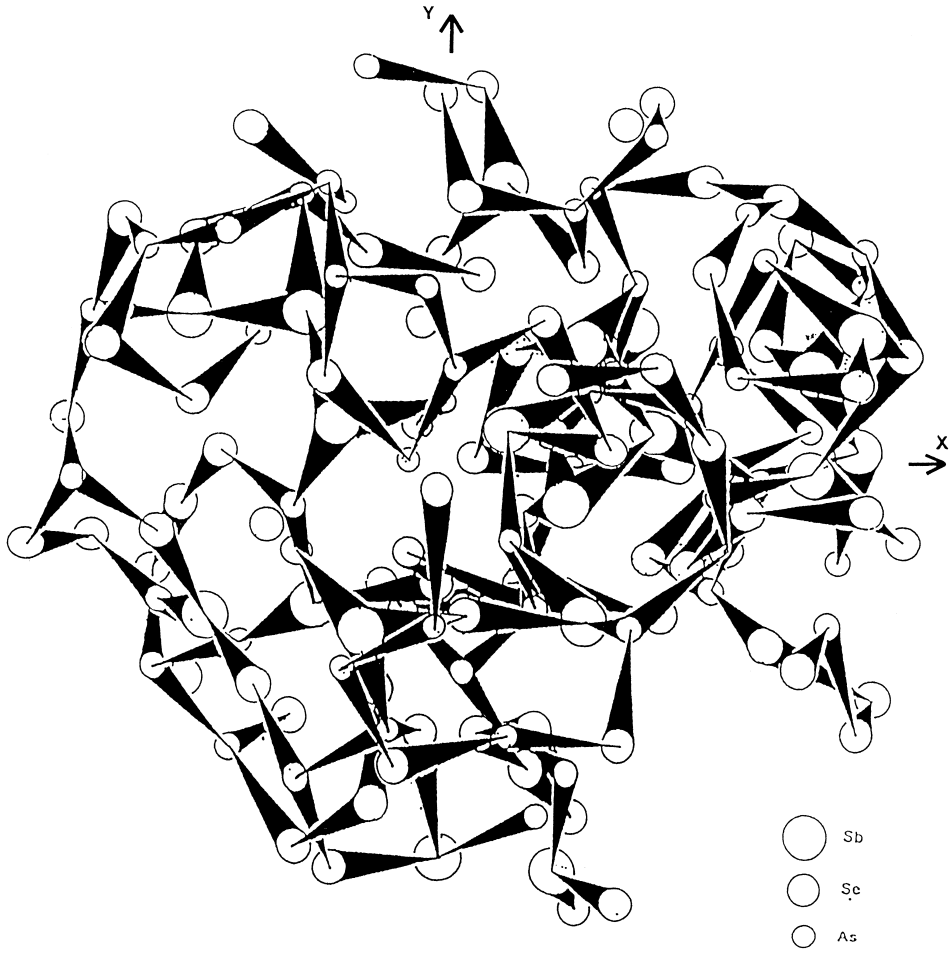

Fig. 4. Spatial representation of the model of glassy alloy $Sb_{0.05}As_{0.45}Se_{0.50}$.

nature of the model. In this case, 65% of unsaturated atoms are less than 2 Å away from the spherical surface, and cannot therefore be considered infracoordinated, as they can bond with external atoms.

As to the bond distances deduced from the model, a good agreement is observed with those quoted in the literature for the same atomic pairs, in alloys similar to the one under study, as reported in Table 4.

Table 4
Averaged bonding distances (Å)

Pair	Bond length	
	This work	Literature
Sb–Sb	2.72	2.80 [10]
Sb–As	2.53	2.60 [10]
Sb–Se	2.48	2.56 [10]
As–As	2.45	2.47 [22]
As–Se	2.44	2.42 [23]
Se–Se	2.45	2.43 [24]

Table 5
Averaged bonding angles (degrees)

Element	Bond angle	
	This work	Literature
Sb	110.39	111.01 [25]
As	108.32	109.81 [20]
Se	108.20	108.82 [25]

5. Conclusions

The percentage of infra-coordinated atoms which are near the spherical surface of the model and which may be saturated with atoms outside it, as well as the average bond angles and the average bond distances deduced for the different pairs of atoms, in relation to the values quoted for them in the literature, in analogous glassy alloys, allow us to state that the generated model is a good statistical representation of the analyzed sample, thus confirming the validity of the Monte Carlo method for the generation of atomic structure models in alloys of chalcogenide glasses.

According to the radial atomic distribution function of the alloy studied, obtained from X-ray diffraction data, and with the consideration of three-coordinated antimony, quoted in the literature, it was possible to correctly explain the average number of first neighbours experimentally determined for the compound in question.

By using the most approximate expression of the area under the first RDF peak, it was possible to find a number of Se–Se bonds for three-coordinated antimony, which, while keeping the coordination numbers n_{22} and n_{23} positive, gives a theoretical area within the margin of error of the experimental area.

The hypothesis of three-coordinated antimony is confirmed by the structural model obtained, in which one may observe basic units made up of triangular pyramids, in one of whose vertices there is an antimony atom. These basic units are joined together directly, or by lateral chains, made up of di-coordinated selenium atoms.

Acknowledgements

The authors are grateful to the Junta de Andalucía for their financial support.

References

[1] N.F. Mott, E.A. Davis, Electronic Processes in Noncrystalline Materials, Clarendon Press, Oxford, 1979.
[2] F. Buda, G.L. Chiarotti, I. Stich, R. Car, M. Parrinello, J. Non-Cryst. Solids 114 (1989) 7.
[3] J. Vázquez, L. Esquivias, P. Villares, R. Jiménez-Garay, An. Fis. B 81 (1985) 223.
[4] J. Vázquez, P. Villares, R. Jiménez-Garay, Mater. Lett. 4 (1986) 485.
[5] J. Vázquez, M. Casas-Ruiz, R.A. Ligero, R. Jiménez-Garay, Mater. Chem. Phys. 32 (1992) 63.
[6] J. Vázquez, F. Sanz, An. Fis. B 80 (1984) 31.
[7] B.E. Warren, X-ray Diffraction, Addison-Wesley, Reading, MA, 1969.
[8] A. d'Anjou, F. Sanz, J. Non-Cryst. Solids 28 (1978) 319.
[9] N.J. Shevchick, PhD Thesis, Harvard University, 1972.
[10] L. Pauling, Uniones Químicas, Kapelusz, Buenos Aires, 1969.
[11] G.N. Greaves, E.A. Davis, Philos. Mag. 29 (1974) 1201.
[12] A. Giridhar, S. Mahadevan, J. Non-Cryst. Solids 51 (1982) 305.
[13] S. Mahadevan, A. Giridhar, A.K. Singh, J. Non-Cryst. Solids 88 (1986) 11.
[14] K. Suzuki, M. Misawa, in: R. Evans, P.A. Greenwood (Eds.), Liquids Metals, 1976.
[15] D.E. Polk, J. Non-Cryst. Solids 5 (1971) 365.
[16] F. Lancon, L. Billard, J. Longier, A. Chamberod, J. Phys. F 12 (1982) 259.
[17] L. Billard, F. Lancon, A. Chamberod, J. Non-Cryst. Solids 51 (1982) 291.
[18] M.D. Rechtin, A.L. Renninger, B.L. Averbach, J. Non-Cryst. Solids 15 (1974) 74.
[19] A.L. Renninger, M.D. Rechtin, B.L. Averbach, J. Non-Cryst. Solids 16 (1974) 1.
[20] J. Vázquez, P. Villares, E. Márquez, R. Jiménez-Garay, Mater. Chem. Phys. 25 (1990) 399.
[21] G. Mason, Nature 217 (1968) 733.
[22] J. Vázquez, P. Villares, R. Jiménez-Garay, J. Non-Cryst. Solids 86 (1986) 251.
[23] D. Gómez-Vela, L. Esquivias, C. Prieto, Phys. Status Solidi B 169 (1992) 303.
[24] J. Vázquez, R.A. Ligero, P. Villares, R. Jiménez-Garay, Mater. Chem. Phys. 26 (1990) 363.
[25] M. Mateos, PhD Thesis, Navarra University, 1983.